

## Band Topology and Linking Structure of Nodal Line Semimetals with $Z_2$ Monopole Charges


Junyeong Ahn,<sup>1,2,3</sup> Dongwook Kim,<sup>4</sup> Youngkuk Kim,<sup>4</sup> and Bohm-Jung Yang<sup>1,2,3,\*</sup>

<sup>1</sup>*Department of Physics and Astronomy, Seoul National University, Seoul 08826, Korea*

<sup>2</sup>*Center for Correlated Electron Systems, Institute for Basic Science (IBS), Seoul 08826, Korea*

<sup>3</sup>*Center for Theoretical Physics (CTP), Seoul National University, Seoul 08826, Korea*

<sup>4</sup>*Department of Physics, Sungkyunkwan University, Suwon 16419, Korea*

 (Received 3 April 2018; revised manuscript received 6 July 2018; published 6 September 2018)

We study the band topology and the associated linking structure of topological semimetals with nodal lines carrying  $Z_2$  monopole charges, which can be realized in three-dimensional systems invariant under the combination of inversion  $P$  and time reversal  $T$  when spin-orbit coupling is negligible. In contrast to the well-known  $PT$ -symmetric nodal lines protected only by the  $\pi$  Berry phase, in which a single nodal line can exist, the nodal lines with  $Z_2$  monopole charges should always exist in pairs. We show that a pair of nodal lines with  $Z_2$  monopole charges is created by a double band inversion process and that the resulting nodal lines are always linked by another nodal line formed between the two topmost occupied bands. It is shown that both the linking structure and the  $Z_2$  monopole charge are the manifestation of the nontrivial band topology characterized by the second Stiefel-Whitney class, which can be read off from the Wilson loop spectrum. We show that the second Stiefel-Whitney class can serve as a well-defined topological invariant of a  $PT$ -invariant two-dimensional insulator in the absence of Berry phase. Based on this, we propose that pair creation and annihilation of nodal lines with  $Z_2$  monopole charges can mediate a topological phase transition between a normal insulator and a three-dimensional weak Stiefel-Whitney insulator. Moreover, using first-principles calculations, we predict  $ABC$ -stacked graphdiyne as a nodal line semimetal (NLSM) with  $Z_2$  monopole charges having the linking structure. Finally, we develop a formula for computing the second Stiefel-Whitney class based on parity eigenvalues at inversion-invariant momenta, which is used to prove the quantized bulk magnetoelectric response of NLSMs with  $Z_2$  monopole charges under a  $T$ -breaking perturbation.

DOI: [10.1103/PhysRevLett.121.106403](https://doi.org/10.1103/PhysRevLett.121.106403)

**Introduction.**—Topological semimetals [1–38] are novel states of matter whose band structure features gap-closing points or lines. Such gapless nodal points or lines are protected by either crystalline symmetry [4–17] or topological invariants [18–38]. The nodal point (Weyl point) in a Weyl semimetal [31–38] is a representative example of the latter case. Because of the quantized monopole charge, Weyl points always exist in pairs [31–34]. Moreover, pair creation and annihilation of Weyl points can mediate topological phase transitions between a normal insulator (NI) and a topological insulator in three dimensions [31–33,37–40]. Since the origin of the monopole charge is the Berry curvature of complex electronic states, breaking either time reversal  $T$  [31–33] or inversion  $P$  [35–38] is a precondition to host a Weyl point [34].

However, recent theoretical studies have found that, in the presence of  $P$  and  $T$  symmetries, a nontrivial monopole charge can exist, carried by a nodal line (NL), when spin-orbit coupling is negligibly weak [18–23]. Here the monopole charge is a  $Z_2$  number originating from the topology of real electronic states [18–20,23], which is clearly distinct from the integer monopole charge of Weyl points originating from complex electronic states. In fact, recently, spinless

fermions in  $PT$ -symmetric systems have received great attention due to the discovery of semimetals with NLs protected by the  $\pi$  Berry phase [23–26], appearing in various forms, including rings [41–49], crossings [50–53], chains [54–56], links [57–64], knots [63–65], nexus [66–68], and nets [69–71]. However, all the NLs belonging to this class do not carry a  $Z_2$  monopole charge. Because of this, such a NL can exist alone in the Brillouin zone (BZ), which can disappear after shrinking to a point [23]. No candidate material has been predicted to host  $Z_2$ -nontrivial NLs ( $Z_2$ NLs) yet. Although there are preceding theoretical studies on  $Z_2$ NLs [21–23], the generic feature of the associated band structure topology, which is useful to facilitate material discovery, has not been thoroughly studied.

In this Letter, we study topological characteristics unique to a nodal line semimetal (NLSM) with  $Z_2$  monopole charges and propose the first candidate material,  $ABC$ -stacked graphdiyne. In particular, we describe the mechanism for creating  $Z_2$ NLs and the linking structure between them, which originates from the underlying global topological characteristics of real electronic states represented by the second Stiefel-Whitney (SW) class. The linking structure exists between a  $Z_2$ NL near the Fermi energy  $E_F$  and another

NL below  $E_F$ , similar to the linking structure predicted in a 5D Weyl semimetal recently [72]. This demonstrates that, in contrast to the common belief, the topological property of a NLSM is determined not only by the local band structure near crossing points at  $E_F$  but also by the global topological structure of all occupied bands below  $E_F$ .

**Band crossing in  $PT$ -invariant spinless fermion systems.**— $Z_2$ -trivial NLs can be described as follows [23,26]. Since  $(PT)^2 = +1$  in the absence of spin-orbit coupling, the  $PT$  operator can be represented by  $PT = K$ , where  $K$  denotes the complex conjugation. In this basis, the  $PT$  invariance of the Hamiltonian,  $PTH(\mathbf{k})(PT)^{-1} = H(\mathbf{k})$ , requires  $H(\mathbf{k})$  to be real. Then the effective two-band Hamiltonian near a band crossing point can be written as  $H(\mathbf{k}) = f_0(\mathbf{k}) + f_1(\mathbf{k})\sigma_x + f_3(\mathbf{k})\sigma_z$ , where  $\sigma_{x,y,z}$  are the Pauli matrices for the two crossing bands and  $f_{0,1,3}(\mathbf{k})$  are real functions of momentum  $\mathbf{k} = (k_x, k_y, k_z)$ . Because closing the band gap requires only two conditions  $f_{1,3}(\mathbf{k}) = 0$  to be satisfied, whereas there are three independent variables  $k_{x,y,z}$ , the generic shape of band crossing points is a line.

On the other hand, to describe  $Z_2$ NLs, one needs to consider a four-band Hamiltonian as first proposed in [23]. When the reality condition is imposed,  $H(\mathbf{k})$  can include three  $4 \times 4$  anticommuting matrices, which indicates that a 3D massless Dirac fermion can exist. The Dirac point is stable against the gap opening because the mass terms, which are imaginary, are forbidden. However, there are other allowed real matrix terms that can deform the Dirac point into a NL. For instance, let us consider the following Hamiltonian introduced in [23],

$$H(\mathbf{k}) = k_x\sigma_x + k_y\tau_y\sigma_y + k_z\sigma_z + m\tau_z\sigma_z, \quad (1)$$

where  $\tau_{x,y,z}$  and  $\sigma_{x,y,z}$  are Pauli matrices. The energy eigenvalues are  $E = \pm\sqrt{k_x^2 + (\rho \pm |m|)^2}$ , where  $\rho = \sqrt{k_y^2 + k_z^2}$ . One can see that the conduction and valence bands touch along the closed loop (a  $Z_2$ NL) satisfying  $k_x = 0$  and  $\rho = |m|$ . Moreover, two occupied bands cross along another line along  $\rho = 0$  (NL\*), which is linked with the  $Z_2$ NL. Because of this linking, the  $Z_2$ NL is stable and distinct from trivial NLs. As  $m \rightarrow 0$ , the linking requires that the  $Z_2$ NL shrinks to a Dirac point. As  $m$  becomes finite after sign reversal, the size of the  $Z_2$ NL increases again. It can never disappear by itself. Because a single  $Z_2$ NL is stable, only a pair of  $Z_2$ NLs can be created by band inversions.

**$Z_2$ NLs in  $ABC$ -stacked graphdiyne.**—Our first-principles calculations predict that  $ABC$ -stacked graphdiyne realizes  $Z_2$ NLs with the linking structure.  $ABC$ -stacked graphdiyne is an  $ABC$  stack of 2D graphdiyne layers composed of a  $sp^2$ - $sp$  carbon network of benzene rings connected by ethynyl chains. [See Fig. 1(c).] Recently, Nomura *et al.* [73] theoretically proposed  $ABC$ -stacked graphdiyne as a NLSM. Here we show that the NLs in this

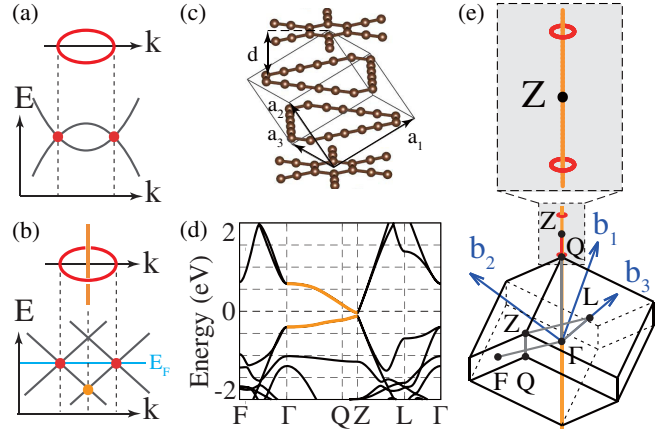


FIG. 1. (a) Band structure near a NL with zero  $Z_2$  monopole charge. (b) Band structure near a NL carrying a unit  $Z_2$  monopole charge ( $Z_2$ NL) linked with another nodal line (NL\*) below the Fermi level ( $E_F$ ). (c) Atomic structure of  $ABC$ -stacked graphdiyne. (d) Band structure of  $ABC$ -stacked graphdiyne where thick orange lines indicate degenerate NLs above and below  $E_F$ . (e) The shape of two  $Z_2$ NLs (red loops) at  $E_F$  ( $E = 0$ ) linked with a NL\* below  $E_F$  (yellow line) in  $ABC$ -stacked graphdiyne. Here, for clarity, only the NL\* linked with  $Z_2$ NLs is shown whereas other unlinked NL\*s are not plotted.

material are  $Z_2$ NLs. Consistent with [73], we find NLs occurring off the high-symmetry  $Z$  point of the BZ. While the electronic band structure displays the band gap along the high-symmetry lines as shown in Fig. 1(d), the valence and conduction bands cross off the high-symmetry  $\mathbf{k}$  points along a pair of closed NLs colored in red in Fig. 1(e). Additionally, we find that two topmost occupied bands form another NL [the orange line in Fig. 1(e)], which pierces the red NLs, manifesting the proposed linking structure. Interestingly, the effective four-band Hamiltonian describing  $ABC$ -stacked graphdiyne near  $E_F$  is identical to Eq. (1) [73], indicating the generality of our theory.

**Double band inversion.**—Let us illustrate a generic mechanism for a pair creation of  $Z_2$ NLs in inversion symmetric systems, which is composed of consecutive band inversions, dubbed a double band inversion (DBI). For concreteness, we describe a DBI by using the Hamiltonian in Eq. (1) after the replacement  $k_z \rightarrow |\mathbf{k}|^2 - M$ . The evolution of the band structure during the DBI is illustrated in Fig. 2(a) as a function of the parameter  $M$ . As we increase  $M$  from  $M < -|m|$ , the first band inversion occurs at  $M = -|m|$  between the top valence and bottom conduction bands, creating a trivial NL. Then, the inversion at  $M = 0$  between two occupied (unoccupied) bands generates another NL below (above)  $E_F$ , which we call NL\*. The last band inversion at  $M = |m|$  between two inverted bands near  $E_F$  splits the trivial NL into two  $Z_2$ NLs linked by the NL\* below  $E_F$  [Fig. 2(a)]. During the DBI, each occupied (unoccupied) band crosses both of two unoccupied (occupied) bands, which explains why the

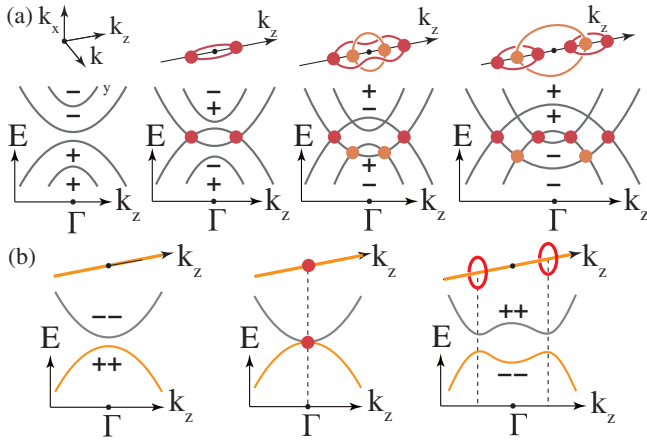


FIG. 2. (a) Evolution of band structure during a double band inversion (DBI). Red (Orange) points and lines indicate the crossing between the conduction and valence bands (two occupied bands).  $\pm$  indicate the inversion eigenvalues at the  $\Gamma$  point. (b) A variant of BDI process realized in graphdiyne. Because of the threefold rotation symmetry, both the valence and conduction bands are degenerate along the  $k_z$  axis; thus  $NL^*$  exists before  $Z_2NL$ s are created.

minimal number of bands required to create a  $Z_2NL$  is four. In  $ABC$ -stacked graphdiyne, both valence and conduction bands are doubly degenerate along the high-symmetry  $k_z$  axis due to threefold rotation symmetry; thus,  $NL^*$  exists from the beginning. In such a system, a single band crossing immediately inverts two occupied and two unoccupied bands having opposite parities, generating a  $Z_2NL$  pair as shown in Fig. 2(b). In noncentrosymmetric systems,  $Z_2NL$  pair creation occurs in a similar manner, that is, by splitting a trivial  $NL$  into a  $Z_2NL$  pair, which are linked with another  $NL$  below  $E_F$  as described in the Supplemental Material [74].

*$Z_2$  monopole charge, linking number, and the second Stiefel-Whitney class.*—Here we give a formal proof for the equivalence between the  $Z_2$  monopole charge and the linking number, based on the correspondence between the  $Z_2$  monopole charge and the second SW class implied by  $K$  theory [95].

The  $Z_2$  invariant was originally defined in [23] as follows. First, we take real occupied states by imposing  $PT|u_{n\mathbf{k}}\rangle = |u_{n\mathbf{k}}\rangle$ . Then we consider a sphere surrounding a  $NL$ , which is divided into two patches (the northern and southern hemispheres) overlapping along the equator as shown in Fig. 3(a). One can find smooth real states  $|u_{n\mathbf{k}}^N\rangle$  ( $|u_{n\mathbf{k}}^S\rangle$ ) on the northern (southern) hemisphere. On the overlapping circle,  $|u_{n\mathbf{k}}^N\rangle$  are connected by a smooth transition function  $t^{NS}(\mathbf{k}) \in SO(N_{\text{occ}})$  in a way that  $|u_{n\mathbf{k}}^S\rangle = t_{mn}^{NS}(\mathbf{k})|u_{m\mathbf{k}}^N\rangle$ , where  $N_{\text{occ}}$  denotes the number of occupied bands. Let us note that, since the real occupied states are orientable on a sphere, transition functions can be restricted to  $SO(N_{\text{occ}})$  [74]. The homotopy group  $\pi_1[SO(N_{\text{occ}} > 2)] = Z_2$  indicates that there is a  $Z_2$ -type

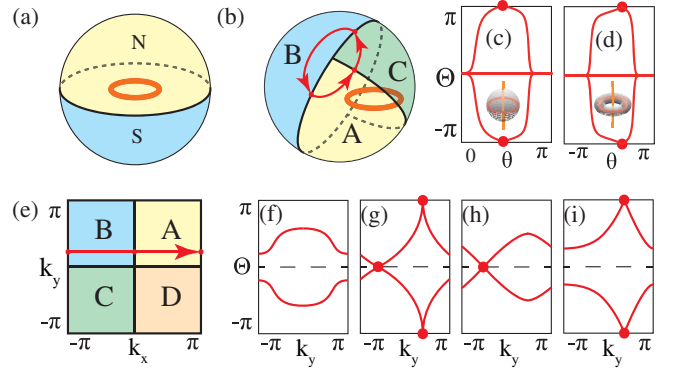


FIG. 3. (a),(b) The wrapping sphere covered by two or three patches. (c),(d) Wilson loop spectrum for  $ABC$ -stacked graphdiyne computed on a sphere or a torus wrapping a  $Z_2NL$ . (e) A torus covered by four patches. (f) The Wilson loop spectrum on a torus with  $(w_{1,y}, w_2) = (0, 0)$  when  $N_{\text{occ}} = 2$ . Similar spectra with  $(w_{1,y}, w_2) = (0, 1), (1, 0), (1, 1)$  are shown in (g)–(i), respectively.

obstruction for defining a real smooth state on the sphere, which is nothing but the  $Z_2$  monopole charge of  $NL$ s. Because  $\pi_1[SO(2)] = Z$ , the winding number of  $t^{NS}(\mathbf{k})$  is an integer invariant when  $N_{\text{occ}} = 2$ . In this case, the  $Z_2$  monopole charge is defined by the parity of the winding number.

Now we make a connection between the  $Z_2$  monopole charge and the second SW class  $w_2$ .  $w_2$  characterizes the obstruction to lifting transition functions of real occupied states to their double covering group [96–98]. When  $w_2 = 0$  ( $w_2 = 1$ ), the lifting is allowed (forbidden). For simplicity, let us first consider the case with  $N_{\text{occ}} = 2$  so that the transition function  $t^{NS}(\mathbf{k}) = \exp[i\theta(\mathbf{k})\sigma_y]$ , where  $\sigma_{x,y,z}$  are the Pauli matrices for two occupied bands. When the  $Z_2$  monopole charge on the sphere is 0 (1), the angle  $\theta(\mathbf{k})$  evolves from 0 to  $4n\pi$  [ $(4n + 2)\pi$ ] with an integer  $n$ , because  $t^{NS}$  is periodic along the equator and has an even (odd) winding number. Now let us ask whether it is possible to take a lift  $t^{NS} \rightarrow \tilde{t}^{NS}$  from  $SO(2)$  to its double covering group  $U(1)$  while the periodicity of  $\tilde{t}^{NS}$  is kept. To answer this, one defines a two-to-one mapping  $\pi: U(1) \rightarrow SO(2)$  by using  $\tilde{t}^{NS}(\theta) = \exp[i\theta/2]$  and  $t^{NS}(\theta) = \exp[i\theta\sigma_y]$ . Let us note that, when  $t^{NS}(\theta)$  has an even (odd) winding number with  $\theta \in [0, 4n\pi]$  ( $\theta \in [0, (4n + 2)\pi]$ ),  $\tilde{t}^{NS}(\theta)$  is periodic (nonperiodic); thus the lifting from  $t^{NS}$  to  $\tilde{t}^{NS}$  is well defined (ill defined). The same argument applies to the case with  $N_{\text{occ}} > 2$  [97]. The  $Z_2$  monopole charge is thus identified with  $w_2$ .

To derive the equivalence between  $w_2$  and the linking number, let us continuously deform the sphere wrapping a  $NL$   $\gamma$ , by gluing the north and south poles at the center, into a thin torus completely enclosing  $\gamma$ . As long as the band gap remains finite during the deformation,  $w_2$  is invariant since the gluing of the north and south poles does not create a

monopole, which is further confirmed numerically as shown in Figs. 3(c) and 3(d). We assume that the torus is thin enough so that all occupied bands on it are nondegenerate. In this limit, according to the Whitney sum formula [99,100],  $w_2$  satisfies the following relations modulo two [74]

$$w_2 = \sum_{n < m} [w_{1,\phi}(\mathcal{B}_n)w_{1,\theta}(\mathcal{B}_m) - w_{1,\phi}(\mathcal{B}_m)w_{1,\theta}(\mathcal{B}_n)], \quad (2)$$

where  $w_{1,\phi}(\mathcal{B}_n)$  and  $w_{1,\theta}(\mathcal{B}_n)$  are the first SW classes of the  $n$ th occupied band  $\mathcal{B}_n$  along the toroidal and poloidal cycle, respectively, on the torus wrapping  $\gamma$ . As shown in the Supplemental Material [74], the first SW classes  $w_{1,\phi}(\mathcal{B}_n)$  and  $w_{1,\theta}(\mathcal{B}_n)$  correspond to the Berry phase  $\Phi_{n,\phi}$  and  $\Phi_{n,\theta}$  of the  $n$ th band along  $\phi$  and  $\theta$  cycles, respectively, calculated in a smooth complex gauge, and it characterizes the orientability of the occupied states. Through a direct calculation of the Berry phase in a Coulomb gauge, we find that [74]

$$w_2 = \sum_{\tilde{\gamma}_j} \text{Lk}(\gamma, \tilde{\gamma}_j), \quad (3)$$

where  $\text{Lk}(\gamma, \tilde{\gamma}_j) = (1/4\pi) \oint_{\gamma} d\mathbf{k} \times \oint_{\tilde{\gamma}_j} d\mathbf{p} \cdot (\mathbf{k} - \mathbf{p})/|\mathbf{k} - \mathbf{p}|^3$  is the linking number [101] between  $\gamma$  and another NL  $\tilde{\gamma}_j$  formed by the occupied band degeneracy. Let us notice that NLs formed between unoccupied bands do not contribute to the linking number (Lk) because the monopole charge is defined by occupied bands. For the model in Eq. (1) with  $N_{\text{occ}} = 2$ ,  $\Phi_{1,\phi} = \pi$ ,  $\Phi_{1,\theta} = \pi$ ,  $\Phi_{2,\phi} = \pi$ , and  $\Phi_{2,\theta} = 0$ , so  $\text{Lk} = 1$  as expected.

*Wilson loop method for computing  $w_2$ .*— $w_2$  can be computed efficiently by using the Wilson loop technique [22,23,102–104]. The relation between the Wilson loop spectrum and the  $Z_2$  monopole charge can be proved by using the definition of  $w_2$  [96,98] as explicitly shown in the Supplemental Material [74]. In general, on a 2D closed manifold with coordinates  $(\phi, \theta)$ , the Wilson loop operator along  $\phi$  at a fixed  $\theta$  is defined by [102–104]  $W_{(\phi_0+2\pi,\theta)\leftarrow(\phi_0,\theta)} = \lim_{N \rightarrow \infty} F_{N-1} F_{N-2} \dots F_1 F_0$ , where  $F_j$  is the overlap matrix at  $\phi_j = \phi_0 + 2\pi j/N$  with matrix elements  $[F_j]_{mn} = \langle u_m(\phi_{j+1}, \theta) | u_n(\phi_j, \theta) \rangle$ , and  $\phi_N = \phi_0$ . On the wrapping sphere covered by three patches, shown in Fig. 3(b), the Wilson loop operator  $W_0(\theta) \equiv W_{(2\pi,\theta)\leftarrow(0,\theta)}$  becomes  $W_0(\theta) = t^{AB} W_{(2\pi,\theta)\leftarrow(\pi,\theta)} t^{BC} \times W_{(\pi,\theta)\leftarrow(\pi/2,\theta)} t^{CA} W_{(\pi/2,\theta)\leftarrow(0,\theta)}$ , where  $t_{mn}^{AB} = \langle u_m^A(0, \theta) | u_n^B(2\pi, \theta) \rangle$ ,  $t_{mn}^{BC} = \langle u_m^B(\pi, \theta) | u_n^C(\pi, \theta) \rangle$ , and  $t_{mn}^{CA} = \langle u_m^C(\pi/2, \theta) | u_n^A(\pi/2, \theta) \rangle$ . Let us take a parallel-transport gauge defined by  $|u_{p;n}^\alpha(\phi, \theta)\rangle = [W_{(\phi,\theta)\leftarrow(\phi_0^{\alpha},\theta)}^\alpha]_{mn} |u_m^\alpha(\phi, \theta)\rangle$ , where  $\phi_0^\alpha = 0, \pi, \pi/2$  for  $\alpha = A, B, C$ , respectively, and  $W^\alpha$  is defined with smooth states within the patch  $\alpha$ . Then the Wilson loop operator becomes

$$W_0(\theta) = W_{p,0}(\theta) = t_p^{AB}(\theta) t_p^{BC}(\theta) t_p^{CA}(\theta), \quad (4)$$

where  $W_p$  and  $t_p$  are the Wilson loop operator and the transition function in the parallel-transport gauge. Let us note that, in this gauge,  $W_0(\theta)$  is simply given by the product of transition functions along the  $\phi$  cycle. Since  $W_0(0, \pi) = 1$  due to the consistency condition at triple overlaps [74], the image of the map  $W_0(\theta)$  for  $\theta \in [0, \pi]$  forms a closed loop. Then  $w_2$  is given by the parity of the winding number of  $W_0(\theta)$  [74], which can be obtained gauge invariantly from its eigenvalue  $\Theta(\theta)$  [22,102]. We apply the Wilson loop technique to  $ABC$ -stacked graphdiyne and find that the  $Z_2$ NLs carry nontrivial monopole charges. Figure 3(c) shows the first-principles calculations of the Wilson loop spectrum computed on a sphere wrapping a  $Z_2$ NL. The single crossing on the  $\Theta = \pi$  line indicates the odd winding number, leading to  $w_2 = 1$ . Figure 3(d) shows that the Wilson loop spectrum computed on a torus is also nontrivial. These first-principles results confirm the NLSM phase that we proposed here hosted in  $ABC$ -stacked graphdiyne.

*2D SW insulator.*—Using  $w_2$  computed on a 2D BZ torus, we can define a new  $PT$ -invariant 2D topological insulator characterized by  $w_2$  when  $w_1 = 0$  (i.e.,  $w_{1,\phi} = w_{1,\theta} = 0$ ). To prove this, we consider a 2D BZ torus with coordinates  $(\phi, \theta) = (k_x, k_y)$  [Fig. 3(e)]. Then  $w_2$  is again given by the spectral degeneracy of the Wilson loop  $W_0(\theta)$  on the torus, as shown in the Supplemental Material [74].

Let us first consider the  $N_{\text{occ}} = 2$  case. We calculate  $W_0$  along an orientable cycle, because otherwise the Wilson loop spectrum has no stable crossing points, such that it does not show the topological property. One can always choose such an orientable cycle [74]. Then, there are four  $Z_2$  homotopy classes of Wilson loop spectra shown in Figs. 3(f)–3(i). They are classified by the parity of the number of linear crossing points on  $\Theta = 0$  and  $\Theta = \pi$ . A spectrum corresponds to  $w_2 = 0$  ( $w_2 = 1$ ) when it has even (odd) linear crossing points on  $\Theta = \pi$ . Figures 3(f)–3(i) are distinguished by the total number of linear crossing points, which is even (odd) since  $w_{1,\theta} = 0$  ( $w_{1,\theta} = 1$ ) [74].

Notice that the topology of the spectrum in Figs. 3(h) and 3(i) differs only by an overall shift of the eigenvalues by  $\pi$ , whereas those in Figs. 3(f) and 3(g) are invariant under the shift. This indicates that  $w_2$  is independent (dependent) of the unit cell choice when  $w_{1,\theta} = 0$  ( $w_{1,\theta} = 1$ ), because the Wilson loop eigenvalues correspond to the Wannier centers for insulators [102]. Indeed, the same unit cell dependence exists for any even  $N_{\text{occ}}$ , whereas  $w_2$  is independent of the unit cell choice for any odd  $N_{\text{occ}}$  [74]. Therefore,  $w_2$  is a well-defined topological invariant when  $w_1 = 0$ . We may call the insulator characterized by  $w_2 = 1$  as a 2D SW insulator (SWI). This is a new kind of fragile topological phase [105–107] since it can be trivialized when bands with  $(w_1, w_2) = (1, 0)$  are added.

*Topological phase transition.*—As a sphere wrapping a  $Z_2$ NL can be continuously deformed to two parallel 2D BZs, one with  $w_2 = 1$  and the other with  $w_2 = 0$ , a  $Z_2$ NL can be considered as a critical state separating a 2D NI and a 2D SWI. Accordingly, the pair creation and annihilation of  $Z_2$ NLs can mediate a topological phase transition between a 3D NI and a 3D weak SWI, a vertical stacking of 2D SWIs. The presence of two NL\* s formed between occupied bands clearly distinguishes a 3D weak SWI from a NI. Interestingly, first-principles calculations show that ABC-stacked graphdiyne turns into a 3D weak SWI after pair annihilation of  $Z_2$ NLs under about 3% of a uniaxial tensile strain applied along the  $z$  direction (see the Supplemental Material [74]).

*Discussion.*—Let us discuss measurable properties of NLSM with  $Z_2$ NLs. Unfortunately, its surface states are generally not robust due to  $P$  breaking on the surface [23]. Nevertheless, our study suggests that observing the linking structure using angle-resolved photoemission spectroscopy [108] can provide strong evidence for  $Z_2$ NLs. Moreover, the bulk magnetoelectric response under a magnetic field can provide another evidence. When  $P$  and  $T$  are individually symmetries of the system, the number of pairs of  $Z_2$ NLs ( $N_{mp}$ ) can be determined from the inversion eigenvalues of the occupied bands at inversion-invariant momenta (IIM). Since a DBI changes two inversion eigenvalues at an IIM,  $N_{mp}$  is given by the sum of the number of negative eigenvalue pairs over all IIM [21,74]. Let us note that, in  $P$ -invariant insulators with broken  $T$ , two times magnetoelectric polarizability  $2P_3$  is determined by inversion eigenvalues in the same way as  $N_{mp}$  is [85]. This implies that a NLSM with an odd number of  $Z_2$ NL pairs turns into an axion insulator, which can host chiral hinge modes along the domain wall [109–111], when the band gap is opened due to a  $T$ -breaking perturbation such as magnetic field [74]. We believe that the theoretical prediction given in the present Letter can be experimentally tested in ABC-stacked graphdiyne in the near future.

J. A. was supported by IBS-R009-D1. B.-J. Y. was supported by the Institute for Basic Science in Korea (Grant No. IBS-R009-D1) and Basic Science Research Program through the National Research Foundation of Korea (NRF) (Grant No. 0426-20170012, No. 0426-20180011), the POSCO Science Fellowship of POSCO TJ Park Foundation (No. 0426-20180002), and the U.S. Army Research Office under Grant No. W911NF-18-1-0137. Y. K. was supported by the Institute for Basic Science (IBS-R011-D1) and NRF grant funded by the Korea government (MSIP) (No. S-2017-0661-000). D. K. was supported by Samsung Science and Technology Foundation under Project No. SSTF-BA1701-07 and Basic Science Research Program through NRF funded by the Ministry of Education (NRF-2018R1A6A3A11044335). The computational calculations were performed using the resource of Korea

Institute of Science and Technology Information (KISTI). We appreciate the helpful discussions with Yoonseok Hwang, Sungjoon Park, Eunwoo Lee, Ken Shiozaki, Haruki Watanabe, and Akira Furusaki.

*Note added.*—Recently, fragile topology in  $Z_2$ -nontrivial NLSMs was also explored in [112]; the results of that work are consistent with our conclusions.

\*bjyang@snu.ac.kr

- [1] N. P. Armitage, E. J. Mele, and A. Vishwanath, *Rev. Mod. Phys.* **90**, 015001 (2018).
- [2] C.-K. Chiu, J. C. Y. Teo, A. P. Schnyder, and S. Ryu, *Rev. Mod. Phys.* **88**, 035005 (2016).
- [3] C. Fang, H. Weng, X. Dai, and Z. Fang, *Chin. Phys. B* **25**, 117106 (2016).
- [4] C. Herring, *Phys. Rev.* **52**, 365 (1937).
- [5] B.-J. Yang and N. Nagaosa, *Nat. Commun.* **5**, 4898 (2014).
- [6] B.-J. Yang, T. Morimoto, and A. Furusaki, *Phys. Rev. B* **92**, 165120 (2015).
- [7] Z. K. Liu, J. Jiang, B. Zhou, Z. J. Wang, Y. Zhang, H. M. Weng, D. Prabhakaran, S.-K. Mo, H. Peng, P. Dudin, T. Kim, M. Hoesch, Z. Fang, X. Dai, Z. X. Shen, D. L. Feng, Z. Hussain, and Y. L. Chen, *Nat. Mater.* **13**, 677 (2014).
- [8] M. Neupane, S.-Y. Xu, R. Sankar, N. Alidoust, G. Bian, C. Liu, I. Belopolski, T.-R. Chang, H.-T. Jeng, H. Lin, A. Bansil, F. Chou, and M. Z. Hasan, *Nat. Commun.* **5**, 3786 (2014).
- [9] Z. K. Liu, B. Zhou, Z. J. Wang, H. M. Weng, D. Prabhakaran, S.-K. Mo, Y. Zhang, Z. X. Shen, Z. Fang, X. Dai, Z. Hussain, and Y. L. Chen, *Science* **343**, 864 (2014).
- [10] B. J. Wieder, Y. Kim, A. M. Rappe, and C. L. Kane, *Phys. Rev. Lett.* **116**, 186402 (2016).
- [11] B. Bradlyn, J. Cano, Z. Wang, M. G. Vergniory, C. Felser, R. J. Cava, and B. A. Bernevig, *Science* **353**, aaf5037 (2016).
- [12] S. M. Young and C. L. Kane, *Phys. Rev. Lett.* **115**, 126803 (2015).
- [13] H. Watanabe, H. C. Po, M. P. Zaletel, and A. Vishwanath, *Phys. Rev. Lett.* **117**, 096404 (2016).
- [14] Y. X. Zhao and A. P. Schnyder, *Phys. Rev. B* **94**, 195109 (2016).
- [15] B.-J. Yang, T. A. Bojesen, T. Morimoto, and A. Furusaki, *Phys. Rev. B* **95**, 075135 (2017).
- [16] Z. Wang, A. Alexandradinata, R. J. Cava, and B. Andrei Bernevig, *Nature (London)* **532**, 189 (2016).
- [17] R. Takahashi, M. Hirayama, and S. Murakami, *Phys. Rev. B* **96**, 155206 (2017).
- [18] T. Morimoto and A. Furusaki, *Phys. Rev. B* **89**, 235127 (2014).
- [19] Y. X. Zhao, A. P. Schnyder, and Z. D. Wang, *Phys. Rev. Lett.* **116**, 156402 (2016).
- [20] Y. X. Zhao and Y. Lu, *Phys. Rev. Lett.* **118**, 056401 (2017).
- [21] C. Fang, Z. Song, and T. Zhang, arXiv:1711.11050 [Phys. Rev. X (to be published)].
- [22] T. Bzdušek and M. Sigrist, *Phys. Rev. B* **96**, 155105 (2017).

- [23] C. Fang, Y. Chen, H.-Y. Kee, and L. Fu, *Phys. Rev. B* **92**, 081201(R) (2015).
- [24] G. P. Mikitik and Y. V. Sharlai, *Phys. Rev. Lett.* **82**, 2147 (1999).
- [25] C.-K. Chiu and A. P. Schnyder, *Phys. Rev. B* **90**, 205136 (2014).
- [26] Y. Kim, B. J. Wieder, C. L. Kane, and A. M. Rappe, *Phys. Rev. Lett.* **115**, 036806 (2015).
- [27] L. M. Schoop, M. N. Ali, C. Straßer, A. Topp, A. Varykhalov, D. Marchenko, V. Duppel, S. S. P. Parkin, B. V. Lotsch, and C. R. Ast, *Nat. Commun.* **7**, 11696 (2016).
- [28] M. Neupane, I. Belopolski, M. M. Hosen, D. S. Sanchez, R. Sankar, M. Szlowska, S.-Y. Xu, K. Dimitri, N. Dhakal, P. Maldonado, P. M. Oppeneer, D. Kaczorowski, F. Chou, M. Z. Hasan, and T. Durakiewicz, *Phys. Rev. B* **93**, 201104 (R) (2016).
- [29] J. Ahn and B.-J. Yang, *Phys. Rev. Lett.* **118**, 156401 (2017).
- [30] S. Park and B.-J. Yang, *Phys. Rev. B* **96**, 125127 (2017).
- [31] X. Wan, A. M. Turner, A. Vishwanath, and S. Y. Savrasov, *Phys. Rev. B* **83**, 205101 (2011).
- [32] K.-Y. Yang, Y.-M. Lu, and Y. Ran, *Phys. Rev. B* **84**, 075129 (2011).
- [33] A. A. Burkov and L. Balents, *Phys. Rev. Lett.* **107**, 127205 (2011).
- [34] A. A. Burkov, M. D. Hook, and L. Balents, *Phys. Rev. B* **84**, 235126 (2011).
- [35] B. Q. Lv, H. M. Weng, B. B. Fu, X. P. Wang, H. Miao, J. Ma, P. Richard, X. C. Huang, L. X. Zhao, G. F. Chen, Z. Fang, X. Dai, T. Qian, and H. Ding, *Phys. Rev. X* **5**, 031013 (2015).
- [36] B. Q. Lv, N. Xu, H. M. Weng, J. Z. Ma, P. Richard, X. C. Huang, L. X. Zhao, G. F. Chen, C. Matt, F. Bisti, V. Stokov, J. Mesot, Z. Fang, X. Dai, T. Qian, M. Shi, and H. Ding, *Nat. Phys.* **11**, 724 (2015).
- [37] S. Murakami and S.-i. Kuga, *Phys. Rev. B* **78**, 165313 (2008); S. Murakami, *New J. Phys.* **9**, 356 (2007).
- [38] S. Murakami, M. Hirayama, R. Okugawa, and T. Miyake, *Sci. Adv.* **3**, e1602680 (2017).
- [39] A. M. Turner, Y. Zhang, R. S. K. Mong, and A. Vishwanath, *Phys. Rev. B* **85**, 165120 (2012).
- [40] S. T. Ramamurthy and T. L. Hughes, *Phys. Rev. B* **92**, 085105 (2015).
- [41] L. S. Xie, L. M. Schoop, E. M. Seibel, Q. D. Gibson, W. Xie, and R. J. Cava, *APL Mater.* **3**, 083602 (2015).
- [42] Y.-H. Chan, C.-K. Chiu, M. Y. Chou, and A. P. Schnyder, *Phys. Rev. B* **93**, 205132 (2016).
- [43] Q. Xu, R. Yu, Z. Fang, X. Dai, and H. Weng, *Phys. Rev. B* **95**, 045136 (2017).
- [44] Y. Chen, Y. Xie, S. A. Yang, H. Pan, F. Zhang, M. L. Cohen, and S. Zhang, *Nano Lett.* **15**, 6974 (2015).
- [45] J. Zhao, R. Yu, H. Weng, and Z. Fang, *Phys. Rev. B* **94**, 195104 (2016).
- [46] R. Li, H. Ma, X. Cheng, S. Wang, D. Li, Z. Zhang, Y. Li, and X.-Q. Chen, *Phys. Rev. Lett.* **117**, 096401 (2016).
- [47] H. Huang, J. Liu, D. Vanderbilt, and W. Duan, *Phys. Rev. B* **93**, 201114 (2016).
- [48] M. Hirayama, R. Okugawa, T. Miyake, and S. Murakami, *Nat. Commun.* **8**, 14022 (2017).
- [49] Y. Du, F. Tang, D. Wang, L. Sheng, E.-j. Kan, C.-G. Duan, S. Y. Savrasov, and X. Wan, *npj Quantum Mater.* **2**, 3 (2017).
- [50] H. Weng, Y. Liang, Q. Xu, R. Yu, Z. Fang, X. Dai, and Y. Kawazoe, *Phys. Rev. B* **92**, 045108 (2015).
- [51] R. Yu, H. Weng, Z. Fang, X. Dai, and X. Hu, *Phys. Rev. Lett.* **115**, 036807 (2015).
- [52] M. Zeng, C. Fang, G. Chang, Y.-A. Chen, T. Hsieh, A. Bansil, H. Lin, and L. Fu, [arXiv:1504.03492v1](https://arxiv.org/abs/1504.03492v1).
- [53] S. Kobayashi, Y. Yamakawa, A. Yamakage, T. Inohara, Y. Okamoto, and Y. Tanaka, *Phys. Rev. B* **95**, 245208 (2017).
- [54] T. Bzdusek, Q. S. Wu, A. Regg, M. Sigrist, and A. A. Soluyanov, *Nature (London)* **538**, 75 (2016).
- [55] Q. Yan, R. Liu, Z. Yan, B. Liu, H. Chen, Z. Wang, and Ling Lu, *Nat. Phys.* **14**, 461 (2018).
- [56] V. I. Gavrilenko, A. A. Perov, A. P. Protogenov, R. V. Turkevich, and E. V. Chulkov, *Phys. Rev. B* **97**, 115204 (2018).
- [57] G. Chang, S.-Y. Xu, X. Zhou, S.-M. Huang, B. Singh, B. Wang, I. Belopolski, J. Yin, S. Zhang, A. Bansil, H. Lin, and M. Z. Hasan, *Phys. Rev. Lett.* **119**, 156401 (2017).
- [58] W. Chen, H.-Z. Lu, and J.-M. Hou, *Phys. Rev. B* **96**, 041102 (2017).
- [59] Z. Yan, R. Bi, H. Shen, L. Lu, S.-C. Zhang, and Z. Wang, *Phys. Rev. B* **96**, 041103(R) (2017).
- [60] P.-Y. Chang and C.-H. Yee, *Phys. Rev. B* **96**, 081114 (2017).
- [61] C. Gong, Y. Xie, Y. Chen, H.-S. Kim, and D. Vanderbilt, *Phys. Rev. Lett.* **120**, 106403 (2018).
- [62] Y. Zhou, F. Xiong, X. Wan, and J. An, *Phys. Rev. B* **97**, 155140 (2018).
- [63] M. Ezawa, *Phys. Rev. B* **96**, 041202(R) (2017).
- [64] L. Li, S. Chesi, C. Yin, and S. Chen, *Phys. Rev. B* **96**, 081116(R) (2017).
- [65] R. Bi, Z. Yan, L. Lu, and Z. Wang, *Phys. Rev. B* **96**, 201305 (2017).
- [66] T. T. Heikkilä and G. E. Volovik, *New J. Phys.* **17**, 093019 (2015).
- [67] T. Hyart and T. T. Heikkilä, *Phys. Rev. B* **93**, 235147 (2016).
- [68] Z. Zhu, G. W. Winkler, Q. S. Wu, J. Li, and A. A. Soluyanov, *Phys. Rev. X* **6**, 031003 (2016).
- [69] X. Zhang, Z.-M. Yu, X.-L. Sheng, H. Y. Yang, and S. A. Yang, *Phys. Rev. B* **95**, 235116 (2017).
- [70] X. Feng, C. Yue, Z. Song, Q. S. Wu, and B. Wen, *Phys. Rev. Mater.* **2**, 014202 (2018).
- [71] A. Bouhon and A. M. Black-Schaffer, [arXiv:1710.04871](https://arxiv.org/abs/1710.04871).
- [72] B. Lian and S.-C. Zhang, *Phys. Rev. B* **94**, 041105(R) (2016); **95**, 235106 (2017).
- [73] T. Nomura, T. Habe, R. Sakamoto, and M. Koshino, *Phys. Rev. Mater.* **2**, 054204 (2018).
- [74] See Supplemental Material at <http://link.aps.org/supplemental/10.1103/PhysRevLett.121.106403>, which includes Refs. [75–94], for more details on the Stiefel-Whitney classes, the Wilson loop method, relation between the  $Z_2$  monopole charge and parity eigenvalues, and the band structure of ABC-stacked graphdiyne.
- [75] W. P. Su, J. R. Schrieffer, and A. J. Heeger, *Phys. Rev. Lett.* **42**, 1698 (1979).
- [76] P. Hořava, *Phys. Rev. Lett.* **95**, 016405 (2005).

- [77] E. Witten, *Rev. Mod. Phys.* **88**, 035001 (2016).
- [78] J. R. Munkres, *Topology* (Prentice-Hall, New York, 2000).
- [79] G. E. Bredon and J. W. Wood, *Inventiones Mathematicae* **7**, 83 (1969).
- [80] V. V. Prasolov, *Elements of Combinatorial and Differential Topology* (American Mathematical Society, Providence, 2006).
- [81] I. M. Gel'fand, *Lectures on Linear Algebra*, translated by A. Shenitzer (Interscience Publishers, New York, 1961), p. 124.
- [82] A. A. Soluyanov and D. Vanderbilt, *Phys. Rev. B* **85**, 115415 (2012).
- [83] W. A. Benalcazar, B. A. Bernevig, and T. L. Hughes, *Science* **357**, 61 (2017).
- [84] L. Fu and C. L. Kane, *Phys. Rev. B* **76**, 045302 (2007).
- [85] T. L. Hughes, E. Prodan, and B. A. Bernevig, *Phys. Rev. B* **83**, 245132 (2011).
- [86] H. C. Po, A. Vishwanath, and H. Watanabe, *Nat. Commun.* **8**, 50 (2017); *Sci. Adv.* **4**, eaat8685 (2018).
- [87] Z. Wang, X.-L. Qi, and S.-C. Zhang, *New J. Phys.* **12**, 065007 (2010).
- [88] X.-L. Qi, T. L. Hughes, and S.-C. Zhang, *Phys. Rev. B* **78**, 195424 (2008).
- [89] R. Okugawa and S. Murakami, *Phys. Rev. B* **96**, 115201 (2017).
- [90] R. Li, J. Wang, X.-L. Qi, and S.-C. Zhang, *Nat. Phys.* **6**, 284 (2010).
- [91] H. J. Monkhorst and J. D. Pack, *Phys. Rev. B* **13**, 5188 (1976).
- [92] J. P. Perdew, K. Burke, and M. Ernzerhof, *Phys. Rev. Lett.* **77**, 3865 (1996).
- [93] P. Giannozzi *et al.*, *J. Phys. Condens. Matter* **21**, 395502 (2009).
- [94] A. M. Rappe, K. M. Rabe, E. Kaxiras, and J. D. Joannopoulos, *Phys. Rev. B* **41**, 1227 (1990).
- [95] K. Shiozaki, M. Sato, and K. Gomi, *Phys. Rev. B* **95**, 235425 (2017).
- [96] Y. Chooquet-Bruhat and C. DeWitt-Morette, *Analysis, Manifolds, and Physics, Part II*, 2nd ed. (Elsevier, Amsterdam, 2000).
- [97] R. C. Kirby and L. R. Taylor, *Pin Structures on Low-Dimensional Manifolds*, London Mathematics Society Lecture Notes No. 151 (Cambridge University, Cambridge, 1990), p. 177.
- [98] M. Nakahara, *Geometry, Topology and Physics*, 2nd ed. (Institute of Physics, Bristol, 2003).
- [99] A. Hatcher, Vector Bundles and K-Theory (unpublished), <https://www.math.cornell.edu/~hatcher/VBKT/VBpage.html>.
- [100] A. Hatcher, *Algebraic Topology* (Cambridge University, Cambridge, 2002).
- [101] R. L. Ricca and B. Nipoti, *J. Knot Theory Ramif.* **20**, 1325 (2011).
- [102] R. Yu, X. L. Qi, A. Bernevig, Z. Fang, and X. Dai, *Phys. Rev. B* **84**, 075119 (2011).
- [103] A. Alexandradinata, X. Dai, and B. A. Bernevig, *Phys. Rev. B* **89**, 155114 (2014).
- [104] A. Alexandradinata, Z. Wang, and B. A. Bernevig, *Phys. Rev. X* **6**, 021008 (2016).
- [105] H. C. Po, H. Watanabe, and A. Vishwanath, *arXiv:1709.06551*.
- [106] J. Cano, B. Bradlyn, Z. Wang, L. Elcoro, M. G. Vergniory, C. Felser, M. I. Aroyo, and B. A. Bernevig, *Phys. Rev. B* **97**, 035139 (2018).
- [107] J. Cano, B. Bradlyn, Z. Wang, L. Elcoro, M. G. Vergniory, C. Felser, M. I. Aroyo, and B. A. Bernevig, *Phys. Rev. Lett.* **120**, 266401 (2018).
- [108] V. N. Strocov, M. Shi, M. Kobayashi, C. Monney, X. Wang, J. Krempasky, T. Schmitt, L. Patthey, H. Berger, and P. Blaha, *Phys. Rev. Lett.* **109**, 086401 (2012).
- [109] C. Fang and L. Fu, *arXiv:1709.01929*.
- [110] E. Khalaf, *Phys. Rev. B* **97**, 205136 (2018).
- [111] E. Khalaf, H. C. Po, A. Vishwanath, and H. Watanabe, *arXiv:1711.11589* [*Phys. Rev. X* (to be published)].
- [112] Z. Wang, B. J. Wieder, J. Li, B. Yan, and B. Andrei Bernevig, *arXiv:1806.11116*.